

# Reflective interferometry for optical metamaterial phase measurements

Kevin O'Brien,<sup>1,2</sup> N. D. Lanzillotti-Kimura,<sup>1</sup> Haim Suchowski,<sup>1</sup> Boubacar Kante,<sup>1</sup> Yongshik Park,<sup>1</sup>  
Xiaobo Yin,<sup>1</sup> and Xiang Zhang<sup>1,3,\*</sup>

<sup>1</sup>NSF Nano-scale Science and Engineering Center (NSEC), 3112 Etcheverry Hall, University of California, Berkeley, California 94720, USA

<sup>2</sup>Department of Physics, University of California, Berkeley, California 94720, USA

<sup>3</sup>Materials Science Division, Lawrence Berkeley National Laboratory, 1 Cyclotron Road, Berkeley, California 94720, USA

\*Corresponding author: xiang@berkeley.edu

Received July 3, 2012; revised August 29, 2012; accepted August 31, 2012;  
posted August 31, 2012 (Doc. ID 171861); published September 26, 2012

The unambiguous determination of optical refractive indices of metamaterials is a challenging task for device applications and the study of new optical phenomena. We demonstrate here simple broadband phase measurements of metamaterials using spectrally and spatially resolved interferometry. We study the phase response of a  $\pi$ -shaped metamaterial known to be an analog to electromagnetically induced transparency. The measured broadband interferograms give the phase delay or advance produced by the metamaterial in a single measurement. The presented technique offers an effective way of characterizing optical metamaterials including nonlinear and gain-metamaterial systems. © 2012 Optical Society of America

OCIS codes: 120.3180, 310.6628.

Metamaterials have demonstrated phenomena not thought possible decades ago, such as optical super-resolution and cloaking [1]. As metamaterials are used to study more nonlinear, ultrafast, and gain phenomena, the extraction of index information from intensity measurements and simulations will grow more challenging and error prone, so there is a need for accurate and fast optical phase measurements. Various approaches exist to measure the phase behavior of metamaterials. Researchers have fabricated structures out of or next to the metamaterial, allowing them to observe the effects of the phase in the far field [2–4]. Polarization walkoff interferometry was used for metamaterial and single nanoparticle phase measurements [5–8]. A Michelson interferometer was used to measure the index of a fishnet metamaterial [9]. In this letter, we demonstrate a simple, fast, broadband, and accurate method for measuring the phase of the light transmitted by a metamaterial array based on spatially and spectrally resolved interferometry.

We report a white light interferometer using reflective optics which can measure the phase change induced by a metamaterial across a broad wavelength range, limited only by the light source bandwidth and detector sensitivity. We pass white light through the sample and a reference path then recombine the light on the input slit of an imaging spectrometer with different vertical angles [Fig. 1(b)] in order to produce spatial fringes along the vertical axis of the image plane [Fig. 2(a)]. The positions of the maxima and minima of this interference pattern are proportional to the phase of each wave and the periodicity is proportional to the angle [10]. A change in the optical length of either beam path causes the fringe pattern to shift vertically. This technique is known as spectrally and spatially resolved interferometry (SSRI) [11], and it has seen many applications in the field of ultrafast optics [12–15]. A summary of the history and analysis of the accuracy of the technique is given in [10]. The use of SSRI with reflective focusing optics allows broadband

phase measurements of small scale ( $\sim 50 \mu\text{m}$ ) metamaterial arrays.

We used a reflective Mach-Zehnder interferometer to perform the broadband optical phase measurement on a metamaterial. As the light source we use a supercontinuum laser (Fianium SC450) spanning a wavelength range of 400–2400 nm. In our experiment we split the incident light into a sample and a reference path using a nonpolarizing beamsplitter cube. We focus the light from the sample path onto the metamaterial using a 20 mm effective focal length off-axis parabolic mirror, recollimate the light using a similar parabolic mirror [M1 and M2 in Fig. 1(a)], then reflect the light into the spectrometer using M3. The reference beam is reflected into the spectrometer using mirrors M4 and M5. The difference between the height ( $y$ ) of the two beams at M4 and the distance ( $L$ ) from the spectrometer determines the angle, and thus the periodicity of the fringes. Previous works on SSRI have found that approximately 20 fringes give the highest accuracy [10]. The two beams are then overlapped without focusing onto the input slit of the imaging spectrometer. The image is acquired with an InGaAs

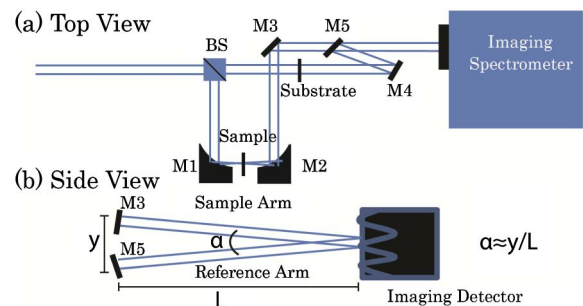


Fig. 1. (Color online) (1) Top and (b) side views of the experimental setup for broadband interferometry. BS, beamsplitter cube; M1, M2: 25 mm focal length  $90^\circ$  off-axis paraboloids; M4 and M5: folding mirrors for the reference path, to produce the angle ( $\alpha$ ) between the sample and reference paths.

infrared camera (SU640KTS-1.7RT,  $640 \times 512$  pixels, with a pitch of  $25 \mu\text{m}$ ) placed at the output port of the spectrometer (angular dispersion of 150 lines/mm and linear dispersion of  $0.5 \text{ nm/pixel}$ ). We set the length of the reference path equal to the length of the sample path and place an identical substrate in the reference path. Typical images of the fringes are shown in Figs. 2(a) and 2(b). Cross sections of the interferograms are shown in Figs. 2(c) and 2(d). We compare interferograms acquired on the sample and adjacent to the sample using a Fourier based technique. We take the Fourier transform (FT) along the vertical axis then find the maximum of the absolute value of the FT, which corresponds to the period of the fringes. The arc tangent of the imaginary divided by real components determines the phase. Subtracting the two results yields the relative phase.

The described technique was used to measure the phase change produced by a  $\pi$ -shaped metamaterial known to produce an optical response analogous to electromagnetically induced transparency (EIT) in atomic systems [16,17] or equivalently a type of Fano resonance [18]. The metamaterial consists of a vertical bar and a pair of horizontal bars which is spaced a varying distance from the vertical bar. Near infrared light can only couple to a bar through the longitudinal plasmon mode associated with the long axis of the bars. In this experiment, we use vertically polarized light which excites a plasmon mode in the vertical bar and in the horizontal bar through near field coupling. The coupling strength between the vertical and horizontal bars can be tuned by changing the distance, and therefore samples with different gap distances have drastically different phase responses. Two gap distances were measured: 10 nm [Fig. 3(a)], corresponding to the blue curve in Figs. 3(c)–3(f), which exhibits a distinct mode splitting and 80 nm [Fig. 3(b)], which has a nearly Lorentzian resonance due to the weak coupling between the bars. The samples were made of

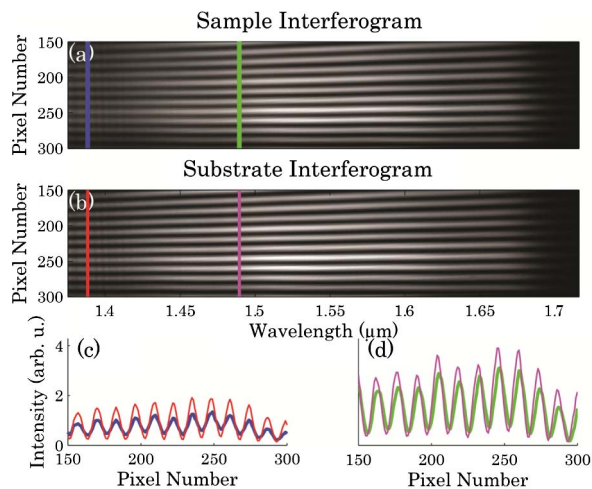


Fig. 2. (Color online) Interferogram obtained for (a) the 80 nm gap sample and for (b) the substrate adjacent to the sample. A  $0.5 \text{ mm}$  quartz substrate is used for the sample and in the reference path. Cross sections are shown at a point where (c) the phase is  $0.0 \text{ rad}$  ( $1.39 \mu\text{m}$ ) and (d)  $0.5 \text{ rad}$  ( $1.49 \mu\text{m}$ ). The difference in the amplitude is due to the absorption of the sample, the power spectrum of the light source, and variations in the detector sensitivity.

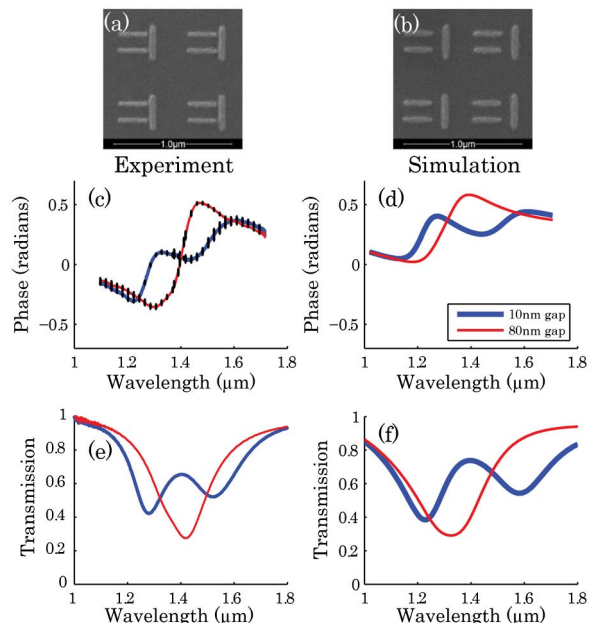


Fig. 3. (Color online) Scanning electron microscope images of the nanostructure arrays with a gap of (a) 10 nm and (b) 80 nm. The dimensions of the vertical bars are  $200 \times 60 \text{ nm}$ , and the horizontal bar  $160 \times 50 \text{ nm}$  with a separation of  $90 \text{ nm}$ . The pitch is  $600 \text{ nm}$  with an array size of  $50 \times 50 \mu\text{m}$ . (c) Measured and (d) simulated phase. (e) The corresponding measured and (f) simulated transmission. The average standard deviation for the phase is  $0.02 \text{ rad}$  ( $\sim \lambda/300$ ).

$35 \text{ nm}$  thick gold deposited with electron beam evaporation and patterned with a standard electron beam lithography and liftoff process. The structure dimensions are given in Fig. 3.

For comparison with the experimental results, we performed numerical simulations of the phase in transmission using the finite element solver Comsol. The simulation was performed with a substrate index of 1.52 with periodic boundary conditions (sample plane) and scattering boundary conditions normal to the plane of the structures, with a domain size of  $0.6 \times 0.6 \times 5 \mu\text{m}$ . In the simulation, we used refractive index data from Johnson and Christy [19] with the damping rate of the gold increased by a factor of three to account for the increased losses due to surface scattering from the rough edges of the nanostructures and grain boundaries in the gold [9]. The structure geometry was scaled by  $+5\%$  to compensate for differences between the designed and fabricated structure. Comparing the experimentally determined phases [Fig. 3(c)] and simulated phases [Fig. 3(d)], one finds a good agreement. A possible explanation for the differences between simulation and experiment is uncertainties in the material parameters and deviations from designed dimensions.

The phase response of the metamaterial array can be understood from the classical light scattering theory. The scattered field has a  $\Pi$  phase change from one side of the resonance to the other, while the phase of the incident field is unchanged [20]. In the far field, the sum of the two fields is measured. The summation is weighted by the scattering cross section, giving a smaller measured phase change further from the resonance where the metamaterial scatters less efficiently. For the weakly

coupled system [Fig. 3(b)] we find a zero crossing in the phase at the same point as the dip in the transmission spectrum. We see a positive phase shift at longer wavelengths and a negative phase shift at shorter wavelengths, consistent with the result for a Lorentz oscillator. In this case, the general shape of the phase curve is similar to the derivative of the transmission with wavelength. For the strongly coupled system, the phase change can no longer be qualitatively understood from the derivative of the transmission with wavelength. Such a model would predict three zero crossings in the phase, due to the three points where the derivative of the transmission is zero. We see only a single zero crossing in both the experiment and simulation. Decreasing the loss of the system would produce the three zero crossings in the phase that are typically found in an EIT-like response [21]. Fabricating the sample from single crystal metals is a potential route to reducing the losses and producing the expected zero crossing [22]. The measured phases allow the calculation of the group delay dispersion (GDD). The maximum and minimum GDD were found on the short and long wavelength sides of the transmission minima with values of  $\pm 200 \text{ fs}^2$  and  $\pm 100 \text{ fs}^2$  for the 80 and 10 nm gap samples, respectively.

When performing multiple measurements, the main difference between consecutive scans is a vertical shift of the phase versus wavelength. The errors for three consecutive measurements are shown in Fig. 3(c) and are 0.02 rad on average. We found the following factors to be important for accurate results: a box around the entire setup to minimize changes in the optical path length of each arm due to air disturbances, smooth substrates, and a large sample area relative to the beam waist. The accuracy of the phase measurements is also influenced by factors such as fringe visibility and uniformity, spatial and spectra resolution, camera noise, and beam uniformity, which are discussed in [10].

In conclusion, we have demonstrated broadband phase measurements of a metamaterial exhibiting EIT in the near infrared with an accuracy of  $\lambda/300$ . This measurement technique will allow rapid and accurate phase characterization of active and nonlinear metamaterials, improving the understanding of these systems and aiding the development of practical metamaterial devices.

This work was supported by the US Department of Energy under contract no. DE-AC02-05CH11231.

## References

1. V. M. Shalaev, *Nat. Photonics* **1**, 41 (2007).
2. J. Valentine, S. Zhang, T. Zentgraf, E. Ulin-Avila, D. A. Genov, G. Bartal, and X. Zhang, *Nature* **455**, 376 (2008).
3. S. Zhang, W. Fan, N. C. Panoiu, K. J. Malloy, R. M. Osgood, and S. R. J. Brueck, *Phys. Rev. Lett.* **95**, 137404 (2005).
4. B. Kanté, J.-M. Lourtioz, and A. de Lustrac, *Phys. Rev. B* **80**, 205120 (2009).
5. V. P. Drachev, W. Cai, U. Chettiar, H.-K. Yuan, A. K. Sarychev, A. V. Kildishev, G. Klimeck, and V. M. Shalaev, *Laser Phys. Lett.* **3**, 49 (2006).
6. E. Pshenay-Severin, F. Setzpfandt, C. Helgert, U. Hübner, C. Menzel, A. Chipouline, C. Rockstuhl, A. Tünnermann, F. Lederer, and T. Pertsch, *J. Opt. Soc. Am. B* **27**, 660 (2010).
7. P. Stoller, V. Jacobsen, and V. Sandoghdar, *Opt. Lett.* **31**, 2474 (2006).
8. M. A. van Dijk, M. Lippitz, and M. Orrit, *Phys. Rev. Lett.* **95**, 267406 (2005).
9. G. Dolling, C. Enkrich, M. Wegener, C. M. Soukoulis, and S. Linden, *Science* **312**, 892 (2006).
10. A. Börzsönyi, A. P. Kovács, M. Görbe, and K. Osvay, *Opt. Commun.* **281**, 3051 (2008).
11. L. Puccianti, *Nuovo Cimento* **5**, 257 (1901).
12. D. Meshulach, D. Yelin, and Y. Silberberg, *J. Opt. Soc. Am. B* **14**, 2095 (1997).
13. D. Meshulach, D. Yelin, and Y. Silberberg, *IEEE J. Quantum Electron.* **33**, 1969 (1997).
14. P. Bowlan, P. Gabolde, A. Shreenath, K. McGresham, R. Trebino, and S. Akturk, *Opt. Express* **14**, 11892 (2006).
15. P. Bowlan, P. Gabolde, M. A. Coughlan, R. Trebino, and R. J. Levis, *J. Opt. Soc. Am. B* **25**, A81 (2008).
16. S. Zhang, D. A. Genov, Y. Wang, M. Liu, and X. Zhang, *Phys. Rev. Lett.* **101**, 047401 (2008).
17. N. Liu, L. Langguth, T. Weiss, J. Kastel, M. Fleischhauer, T. Pfau, and H. Giessen, *Nat. Mater.* **8**, 758 (2009).
18. B. Luk'yanchuk, N. I. Zheludev, S. A. Maier, N. J. Halas, P. Nordlander, H. Giessen, and C. T. Chong, *Nat. Mater.* **9**, 707 (2010).
19. P. B. Johnson and R. W. Christy, *Phys. Rev. B* **6**, 4370 (1972).
20. C. F. Bohren and D. R. Huffman, *Absorption and Scattering of Light by Small Particles* (Wiley-VCH, 1998).
21. M. Fleischhauer, A. Imamoglu, and J. P. Marangos, *Rev. Mod. Phys.* **77**, 633 (2005).
22. J.-S. Huang, V. Callegari, P. Geisler, C. Brünig, J. Kern, J. C. Prangsma, X. Wu, T. Feichtner, J. Ziegler, P. Weinmann, M. Kamp, A. Forchel, P. Biagioni, U. Sennhauser, and B. Hecht, *Nat. Commun.* **1**, 150 (2010).